International Journal of Thermal Sciences 49 (2010) 820–828

Contents lists available at ScienceDirect

International Journal of Thermal Sciences

journal homepage: www.elsevier.com/locate/ijts

Unsteady viscous flows and Stokes's first problem

Y.S. Muzychka [a,*], M.M. Yovanovich [b]

[a] Faculty of Engineering and Applied Science, Memorial University of Newfoundland, St. John's, NL A1B 3X5, Canada
[b] Department of Mechanical Engineering, University of Waterloo, Waterloo, ON N2L 3G1, Canada

ARTICLE INFO

Article history:
Received 29 July 2009
Received in revised form
24 November 2009
Accepted 27 November 2009
Available online 21 December 2009

Keywords:
Viscous flow
Stokes's first problem
Unsteady flow
Couette flow
Poiseuille flow
Blasius flow
Asymptotic modelling
Scaling
MEMS

ABSTRACT

Unsteady viscous flows and Stokes's first problem are examined. Three problems are considered: unsteady Couette flow, unsteady Poiseuille flow, and unsteady boundary layer flow. The relationship between these three fundamental unsteady flows and Stokes' first problem is illustrated. Scaling principles are used to deduce the short time and long time characteristics of these three problems. Asymptotic analysis is used to obtain exact short and long time characteristics and to show the relationship of each problem to Stokes's first problem for short times. Finally, compact robust models are developed for all values of time using the Churchill–Usagi asymptotic correlation method to combine the short and long time characteristics.

1. Introduction

Stokes's first problem is a fundamental solution in fluid dynamics, which represents one of the few exact solutions to the Navier–Stokes equations [1–8]. The problem simply stated, describes the evolution of the velocity field in the vicinity of an infinite plate which is impulsively set in motion with constant velocity, U, in an infinite fluid medium, as shown in Fig. 1. Of primary interest are the rate of penetration, δ, of the velocity field into the fluid and the shear stress at the surface of the plate, τ_w.

Three additional problems can be characterized by the Stokes solution at short times. These are: unsteady Couette flow, unsteady Poiseuille flow, and unsteady boundary layer flow. In the latter case, the boundary layer near the leading edge of a semi-infinite plate will have a characteristic shear stress similar to Blasius flow (or at long times), while downstream (or at short times) the boundary layer is similar to that in Stokes flow. The three problems of interest are shown schematically in Fig. 2.

Each of these problems has been addressed in the fluid literature using analytical, approximate analytical, or numerical solution methods. However, they have not all received adequate attention from the point of view of scaling analysis and asymptotic analysis, nor have simple models been developed for the wall shear stress. In the case of unsteady Poiseuille flow, this problem has recently been addressed by the authors [9]. The key results are included here for completeness.

This paper addresses each of these three problems and develops simple compact models for the dimensionless wall shear stress as a function of dimensionless time. These models are developed by using scaling principles [10] to deduce the correct asymptotic behavior, asymptotic analysis to obtain the exact solutions to the limiting behavior [11], and non-linear superposition to obtain the compact model [12,13]. In all three cases, the compact models are compared with the more complex exact solutions. These models may be used to model the transient fluid behavior in micro-systems (MEMS) involving liquids or gases providing that non-continuum effects are minimal.

Compact models are easily developed using the asymptotic correlation method proposed by Churchill and Usagi [12]. Once the exact asymptotic behavior of a system of interest is known for short and long time, these limits are then combined to develop a simple compact model for the dimensionless quantity of interest. In general form we may write:

$$y^* = \left[\left(y_0^*\right)^n + \left(y_\infty^*\right)^n\right]^{1/n} \tag{1}$$

* Corresponding author.
E-mail address: y.s.muzychka@gmail.com (Y.S. Muzychka).

1290-0729/$ – see front matter © 2009 Elsevier Masson SAS. All rights reserved.
doi:10.1016/j.ijthermalsci.2009.11.013

Nomenclature

A	area, m^2
D_h	hydraulic diameter, $\equiv 4A/P$
h	characteristic channel dimension, m
$J_0(\cdot)$	Bessel function of first kind order zero
$J_1(\cdot)$	Bessel function of first kind order one
L	duct or channel length, m
$\mathcal{L}$	arbitrary length scale, m
m	series index
n	asymptotic correlation parameter, Eqs. (1) and (70)
n	directed normal, m
p	asymptotic correlation parameter, Eq. (71)
p	pressure, *Pa*
P	perimeter, m
$Po_{\mathcal{L}}$	Poiseuille number, $\equiv \tau\mathcal{L}/\mu\overline{w}$
r	radial coordinate, m
s	arc length, m
St	Strouhal number, x/Ut
t	time, s
t^*	dimensionless time, $\equiv \nu t/\mathcal{L}^2$
u	local velocity, m/s
$\overline{u}$	average velocity, m/s
U	surface or stream velocity, m/s
x, y, z	Cartesian coordinates, m
y_0^*	short time asymptote
y_∞^*	long time asymptote
y^*	compact dimensionless model

Greek Symbols

δ	boundary layer thickness, m
δ_s	boundary layer thickness, m
δ_m	boundary layer thickness, m
δ_n	eigenvalue
η	similarity variable
μ	dynamic viscosity, Ns/m^2
ν	kinematic viscosity, m^2/s
ρ	density, kg/m^3
τ_w	wall shear stress, *Pa*

Subscripts

w	wall
0	short time value
∞	long time value
$\mathcal{L}$	based on the arbitrary length $\mathcal{L}$

Superscripts

$\overline{(\bullet)}$	mean value
$(\cdot)^*$	dimensionless value

The correlation parameter n can be either positive or negative. In the case of $n > 0$ the asymptotes are combined to give a concave up function, while for $n < 0$ the asymptotes are combined to give a concave down function. Fig. 3, illustrates the case for $n < 0$.

Once the asymptotes are known, simple criteria for the transition point can easily be determined by finding the intersection of the asymptotes:

$$y_0^* \sim y_\infty^* \tag{2}$$

This expression is then solved in closed form to give the nominal critical value of the independent parameter, which is then used as a transitional criterion. We now proceed to examine the characteristics and solutions of four fundamental problems in unsteady viscous flow.

2. Four fundamental problems

Four fundamental problems in unsteady viscous flow are: Stokes's first problem, unsteady Couette flow, unsteady Poiseuille flow, and unsteady boundary layer flow. Each is discussed from the point of view of scaling, asymptotics, and compact modelling.

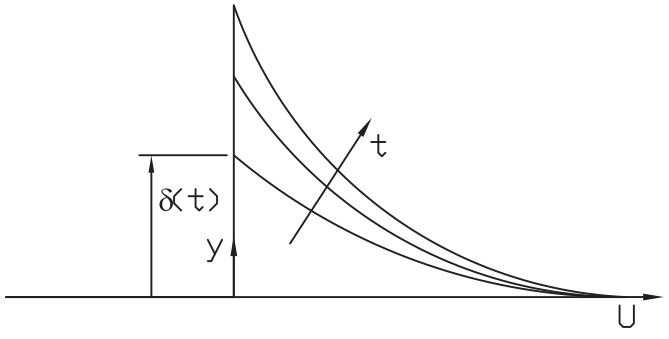

Fig. 1. Stokes's First Problem.

2.1. Stokes's first problem

One of the most important fundamental problems in unsteady viscous flows is that of impulsively started motion of a body in an infinite fluid medium. The simplest problem is that of suddenly setting an infinite flat plate in motion with velocity U. This particular problem is often referred to as Stokes's first problem (Schlichting [2], Currie [3]) and is also referred to in some texts as the Rayleigh problem (Rosenhead [1], Telionis [4], Panton [5]).

The momentum transport problem referred to as Stokes's first problem or Stokes flow [3], requires obtaining the solution to:

$$\frac{\partial u}{\partial t} = \nu \frac{\partial^2 u}{\partial y^2} \tag{3}$$

which is subject to:

$$\left.\begin{array}{ll} y = 0 & u(0,t) = U \\ y \to \infty & u(y \to \infty, t) = 0 \\ t = 0 & u(y,0) = 0 \end{array}\right\} \tag{4}$$

The problem stated above describes viscous diffusion, however analogous problems in heat and mass diffusion exist. The solution is easily obtained in terms of the complementary error function.

Before proceeding to an exact solution, we see that a simple scale analysis can provide much useful information. We assume that $t \sim t$, $u \sim U$, and $y \sim \delta$, where δ is the boundary layer thickness or penetration depth of the flow field. Using these scales we arrive at

$$\frac{U}{t} \sim \nu \frac{U}{\delta^2} \tag{5}$$

or

$$\delta \sim \sqrt{\nu t} \tag{6}$$

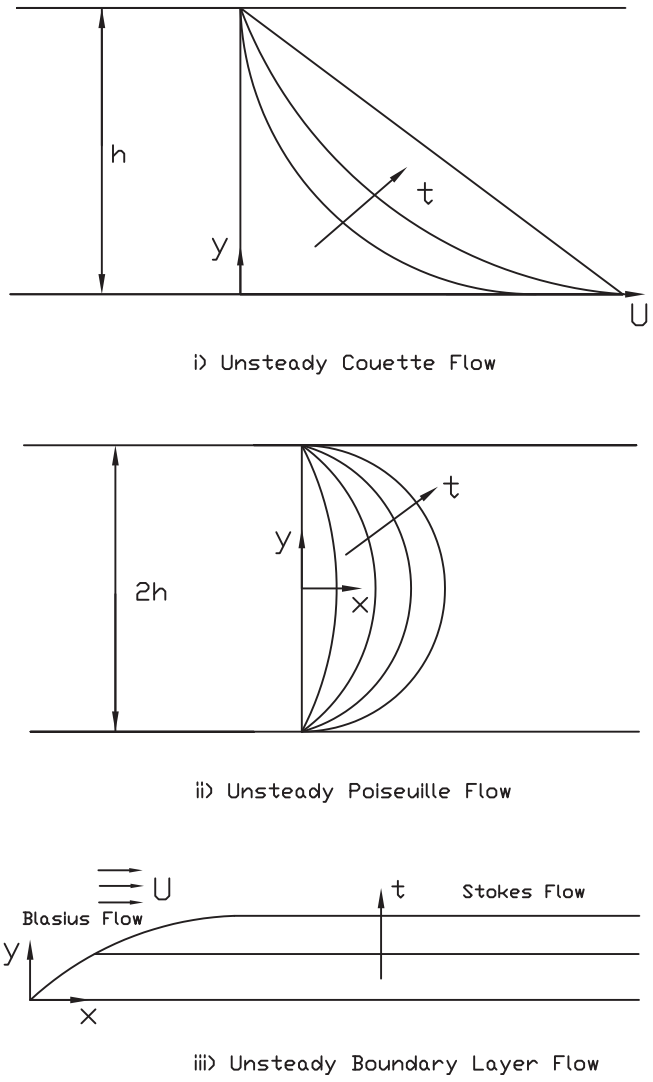

Fig. 2. Three Unsteady Viscous Flow Problems.

for the penetration depth. Problems in semi-infinite domains are of the penetration type, i.e., $\delta \sim \sqrt{\nu t}$ or $\delta \sim \sqrt{\nu x/U}$. The shear stress at the plate surface may be approximately obtained as:

$$\tau_w \sim \frac{\mu U}{\delta} \sim \frac{\mu U}{\sqrt{\nu t}} \tag{7}$$

or, defining a dimensionless shear stress

$$\tau^* \sim \frac{\tau_w \delta}{\mu U} \sim 1 \tag{8}$$

The exact solution is found in terms of the complementary error function [1–8]:

$$\frac{u}{U} = 1 - \mathrm{erf}\left(y/2\sqrt{\nu t}\right) = \mathrm{erfc}\left(y/2\sqrt{\nu t}\right) \tag{9}$$

where $\mathrm{erfc}(\cdot)$ is the *complementary error function*. The solution is readily computed in any mathematical software package.

Finally, it is of interest to determine the drag on the plate. The shear stress is defined as:

$$\tau_w = -\mu \frac{\partial u}{\partial y}\Big|_{y=0} \tag{10}$$

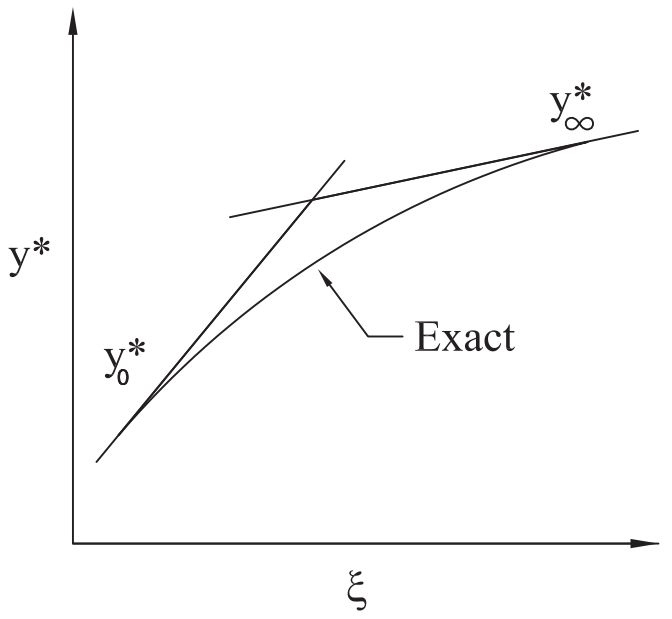

Fig. 3. Asymptotic Model Development.

which becomes:

$$\tau_w = \frac{\mu U}{\sqrt{\pi \nu t}} \tag{11}$$

This result agrees with the scaling analysis except for the factor of $1/\sqrt{\pi}$. We may now define the dimensionless shear stress from Eq. (8)as:

$$\tau^* = \frac{1}{\sqrt{\pi}} \tag{12}$$

The boundary layer thickness may now be obtained using Eq. (9). The approximate value for δ as obtained from Eq. (9) for the case where $u/U = 0.01$ gives:

$$\delta = 3.643\sqrt{\nu t} \tag{13}$$

We may also define two additional measures of boundary layer thickness. One is related to the shear stress through Eq. (11) and gives:

$$\delta_s = \sqrt{\pi}\sqrt{\nu t} \approx 1.772\sqrt{\nu t} \tag{14}$$

and the other relates the total mass of fluid set in motion above the surface of the plate defined as [14]:

$$U\delta_m = \int_0^\infty u\, dy \tag{15}$$

which gives

$$\delta_m = \frac{2}{\sqrt{\pi}}\sqrt{\nu t} \approx 1.128\sqrt{\nu t} \tag{16}$$

The three thicknesses relate to one another according to:

$$\delta_m < \delta_s < \delta \tag{17}$$

Later, we shall see that the δ_m definition plays an important role in the asymptotic results for unsteady Poiseuille flow.

2.2. Unsteady Couette flow

We now re-examine the problem of unsteady Couette flow. Couette flow has been used as the fundamental method for the

measurement of viscosity. Further, it is used in many wall driven applications as means of estimating the drag force. The problem requires solution to the following viscous diffusion equation:

$$\frac{\partial u}{\partial t} = \nu \frac{\partial^2 u}{\partial y^2} \tag{18}$$

subject to:

$$\left.\begin{array}{ll} y = 0 & u(0,t) = U \\ y = h & u(h,t) = 0 \\ t = 0 & u(y,0) = 0 \end{array}\right\} \tag{19}$$

2.2.1. Scale analysis

First, the application of scaling principles for short times shows that the problem is accurately modelled as Stokes flow when

$$\delta \sim \sqrt{\nu t} < h$$

For short time, the wall shear stress scales according to:

$$\tau_0 \sim \frac{\mu U}{\delta} \sim \frac{\mu U}{\sqrt{\nu t}} \tag{20}$$

and for long time it scales according to

$$\tau_\infty \sim \frac{\mu U}{h} \tag{21}$$

We may define a dimensionless wall shear stress as:

$$\tau^* = \frac{\tau_w}{\tau_\infty} \tag{22}$$

This leads to the following results:

$$\left.\begin{array}{ll} \tau^* \sim \dfrac{1}{\sqrt{t^*}} & t^* \to 0 \\ \tau^* \sim 1 & t^* \to \infty \end{array}\right\} \tag{23}$$

where

$$t^* = \frac{\nu t}{h^2} \tag{24}$$

The unsteady Couette flow also has an analogue in transient heat conduction for a plane wall subject to a sudden step change in temperature at one surface. In this case t^* is replaced by the Fourier number, $\alpha t/h^2$.

2.2.2. Asymptotic analysis

The exact solution may be found in the texts of Sherman [6], White [7], or Batchelor [8], and is often reported as:

$$\frac{u}{U} = \left(1 - \frac{y}{h}\right) - 2\sum_{n=1}^{\infty} \frac{\sin(n\pi y/h)}{n\pi} \exp(-n^2\pi^2 \nu t/h^2) \tag{25}$$

The solution for very short times requires many terms to achieve convergence of the velocity field. However, for very short times, the velocity field has not penetrated far enough into the fluid to reach the stationary wall. Thus, the solution governed by Stokes's first problem is valid soon after the flow commences. It is well known that for $t^* \lesssim 0.01$, the field can be represented by Eq. (9).

The shear stress is obtained from:

$$\tau_w = -\mu \frac{\partial u}{\partial y}\Big|_{y=0} \tag{26}$$

which gives:

$$\tau_w = \frac{\mu U}{h}\left(1 + 2\sum_{n=1}^{\infty} \exp(-n^2\pi^2 \nu t/h^2)\right) \tag{27}$$

or defining the dimensionless shear stress τ_w/τ_∞, we obtain

$$\tau^* = 1 + 2\sum_{n=1}^{\infty} \exp(-n^2\pi^2 t^*) \tag{28}$$

where $\tau_\infty = \mu U/h$. The above equation contains the following asymptotes:

$$\left.\begin{array}{ll} \tau^* = \dfrac{1}{\sqrt{\pi}\sqrt{t^*}} & t^* \to 0 \\ \tau^* = 1 & t^* \to \infty \end{array}\right\} \tag{29}$$

which agree with the scaling results in the order of magnitude sense.

2.2.3. Compact model

The dimensionless wall shear may be more easily modelled by considering the asymptotes above and the following equation using the approach of Churchill and Usagi [12] and Eq. (1). Using Eq. (1) with the asymptotes defined by Eq. (29), with at least one known point, one can solve for n. In the present case, we obtain $n \approx 25/3$ to give:

$$\tau^* = \left[\left(\frac{1}{\sqrt{\pi}}\frac{1}{\sqrt{t^*}}\right)^{25/3} + 1\right]^{3/25} \tag{30}$$

which is much more efficient than the series form. The above equation provides accuracy of $\pm$ 0.3 percent. It is plotted in Fig. 4 along with data obtained from Eq. (28). The transition point which may be defined by the intersection of the asymptotes, shows that steady state is obtained when $t^* > 1/\pi \approx 0.3183$.

2.3. Unsteady Poiseuille flow

Unsteady Poiseuille flow is described by the following unsteady momentum equation:

$$\frac{1}{\nu}\frac{\partial u}{\partial t} = -\frac{1}{\mu}\frac{dp}{dz} + \frac{\partial^2 u}{\partial x^2} + \frac{\partial^2 u}{\partial y^2} \tag{31}$$

which is subject to the boundedness condition along the axis of the geometry, $u \neq \infty$, homogeneous Dirichlet conditions at the boundary, $u = 0$, and the initial condition $u = 0$, when $t = 0$. The system is shown in Fig. 2. It consists of an infinitely long duct or

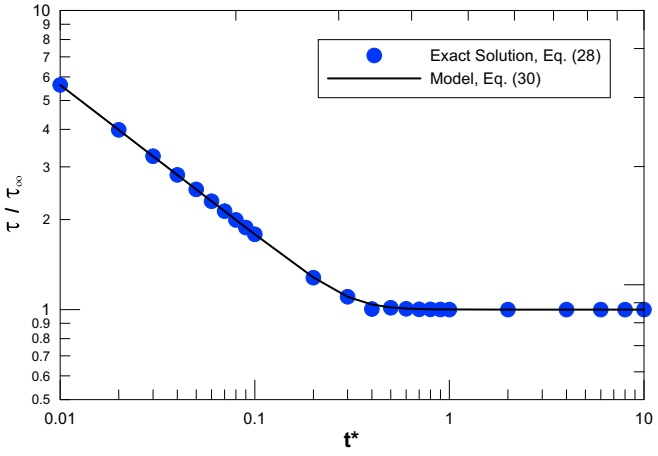

Fig. 4. τ^* for Unsteady Couette Flow.

cylinder of arbitrary but constant cross-sectional area, A, bounded by perimeter, P.

It is of interest to obtain the area mean velocity, obtained by integrating the solution for u over the cross-sectional area:

$$\overline{u}(t) = \frac{1}{A}\iint_A u dA \tag{32}$$

Also, of interest is the perimeter averaged or mean shear stress at the surface:

$$\overline{\tau}_w(t) = \frac{1}{P}\oint \mu\frac{\partial u}{\partial n} ds \tag{33}$$

The dimensionless mean velocity may be defined as:

$$u^* = \frac{\overline{u}}{-\mathcal{L}^2\frac{1}{\mu}\frac{dp}{dz}} \tag{34}$$

while the dimensionless shear stress at the surface is defined with respect to the steady state value:

$$\tau^* = \frac{\overline{\tau}_w}{\tau_\infty} \tag{35}$$

where

$$\tau_\infty = -\frac{A}{P}\frac{dp}{dz} \tag{36}$$

is obtained from the steady state force balance.

2.3.1. Scale analysis

We now examine what information scale analysis provides. Equation (31) represents a balance of three quantities: storage, generation, and diffusion. There are three distinct flow regions in this problem that may be considered. Fully developed flow exists after a very long time, and at short times, there exists a potential core and a very thin boundary layer region. Each of these regions may be analyzed using scale analysis. The following scales will be used: $u \sim \overline{u}$, $t \sim t$, and $\nabla^2 \sim 1/\mathcal{L}^2$ for long time and $\nabla^2 \sim 1/\mathcal{L}^2$ for short time. Here, $\mathcal{L}$ is as yet undetermined characteristic length scale related to the geometry and δ is the boundary layer thickness or penetration scale associated with early times.

First, for long times $t \to \infty$, or fully developed flow, the balance between generation and diffusion leads to:

$$\frac{\overline{u}}{\mathcal{L}^2} \sim \mathcal{G} \tag{37}$$

or

$$\overline{u} \sim \mathcal{G}\mathcal{L}^2 \tag{38}$$

where $\mathcal{G} = -\frac{1}{\mu}\frac{dp}{dz}$. The dimensionless mean velocity becomes:

$$u^* = \frac{\overline{u}}{\mathcal{G}\mathcal{L}^2} \sim 1 \text{ as } t \to \infty \tag{39}$$

Next, for short times $t \to 0$, the balance is between storage and generation, or considering the potential core, this leads to

$$\frac{1}{\nu}\frac{\overline{u}}{t} \sim \mathcal{G} \tag{40}$$

or

$$\overline{u} \sim \mathcal{G}\nu t \tag{41}$$

or

$$u^* \sim \frac{\nu t}{\mathcal{L}^2} \sim t^* \text{ as } t \to 0 \tag{42}$$

Next, in the boundary layer region, the balance between storage and diffusion leads to:

$$\frac{1}{\nu}\frac{\overline{u}}{t} \sim \frac{\overline{u}}{\delta^2} \tag{43}$$

or

$$\delta \sim \sqrt{\nu t} \tag{44}$$

which is the intrinsic penetration depth.

The flow becomes fully developed when $\delta \sim \mathcal{L}$, such that

$$\nu t \sim \mathcal{L}^2 \tag{45}$$

or

$$t^* \sim \frac{\nu t}{\mathcal{L}^2} \sim 1 \tag{46}$$

Finally, we wish to develop expressions for the mean shear stress at the surface defined as:

$$\overline{\tau}_w = \mu\frac{\overline{\partial u}}{\partial n} \tag{47}$$

We must consider the two limiting cases of short time and long time. For long time, $t \to \infty$, the shear stress becomes:

$$\overline{\tau}_w \sim \mu\frac{\overline{u}}{\mathcal{L}} \tag{48}$$

We may also relate the shear stress to the source $\mathcal{G}$ for fully developed flows, where

$$\overline{\tau}_\infty = \frac{A}{P}\mu\mathcal{G} \tag{49}$$

Thus, if we define $\tau^* = \overline{\tau}_w/\tau_\infty$, we obtain

$$\tau^* = \frac{\overline{u}}{\left(\frac{A}{P}\mathcal{G}\mathcal{L}\right)} \sim 1 \quad \text{as} \quad t \to \infty \tag{50}$$

Finally, for short times, $t \to 0$, the shear stress becomes

$$\overline{\tau}_w \sim \frac{\mu\overline{u}}{\delta} \tag{51}$$

Also, from the momentum transport equation we see that

$$\frac{\overline{u}}{\delta^2} \sim \mathcal{G} \tag{52}$$

or, after combining Eqs. (51) and (52):

$$\overline{\tau}_w \sim \mu\mathcal{G}\delta \tag{53}$$

Finally defining τ^* as before, we obtain

$$\tau^* \sim \frac{\delta}{A/P} \sim \frac{\sqrt{t^*}\mathcal{L}}{A/P} \quad \text{as} \quad t \to 0 \tag{54}$$

It is clear from scaling analysis, that two distinct characteristics are present. These are the dimensionless mean velocity, u^* and dimensionless mean shear stress, τ^*. Each has the following asymptotic behavior:

$$\left.\begin{array}{ll} u^* \sim t^* & t^* \to 0 \\ u^* \sim 1 & t^* \to \infty \end{array}\right\} \tag{55}$$

and

$$\left.\begin{array}{ll} \tau^* \sim \sqrt{t^*} & t^* \to 0 \\ \tau^* \sim 1 & t^* \to \infty \end{array}\right\} \tag{56}$$

2.3.2. Asymptotic analysis

The exact asymptotic behavior for small and large times may now be examined for each dimensionless quantity of interest. The authors recently addressed these issues in [9], and only a brief summary is given below.

For long time, $t \to \infty$, the flow is characterized by a balance between generation and diffusion. This problem has been analyzed extensively for momentum transport and solutions to many configurations may be found in the literature and reference books. The results are usually presented in the form of the dimensionless group *fRe*, the *Fanning* friction factor Reynolds number product defined as:

$$\frac{fRe_{\mathcal{L}}}{2} = \frac{\overline{\tau}_\infty \mathcal{L}}{\mu \overline{u}} = Po_{\mathcal{L}} \tag{57}$$

where *Po* is referred to in the fluids literature as the Poiseuille number [7].

We can further introduce the source term through the fully developed flow balance Eq. (36) and obtain:

$$Po_{\mathcal{L}} = \frac{\overline{\tau}_\infty \mathcal{L}}{\mu \overline{u}} = \frac{\frac{A}{P}\mathcal{G}\mathcal{L}}{\overline{u}} \tag{58}$$

Rearranging, for $\overline{u}$ and using the definition of the dimensionless mean velocity, Eq. (34), we obtain

$$u^* = \frac{A/P}{Po_{\mathcal{L}}\mathcal{L}} \tag{59}$$

Finally, by virtue of the definition of the dimensionless shear stress, Eq. (35) and the value for τ_∞, the dimensionless asymptotic limit for τ^* is:

$$\tau^* = 1 \tag{60}$$

For short times, $t \to 0$, the transport is characterized by a balance between generation and storage. The equation of transport which may be solved in the potential core when δ is small is:

$$\frac{1}{\nu}\frac{\partial u}{\partial t} = \mathcal{G} \tag{61}$$

This may be integrated and solved with the initial condition $u(0) = 0$ to give:

$$u(t) = \nu t \mathcal{G} \approx \overline{u}(t) \tag{62}$$

When non-dimensionalized, the solution for short time in the potential core is:

$$u^* = \frac{\nu t}{\mathcal{L}^2} = t^* \tag{63}$$

The short time shear stress may be found by considering the classic Stokes solution for momentum transport in an infinite medium. The solution for the field resulting from a step change at the surface is:

$$u = U\mathrm{erfc}\left(\frac{y}{2\sqrt{\nu t}}\right) \tag{64}$$

The result for the boundary layer thickness which accounts for the mean penetration of the field from the surface to the potential core, i.e. the area under the curve defined by Eq. (64), may be written as [9]:

$$\delta_m U = 2\sqrt{\nu t}\int_0^\infty U\mathrm{erfc}(\eta)\, d\eta \tag{65}$$

where $\eta = y/2\sqrt{\nu t}$, which gives

$$\delta_m = \frac{2}{\sqrt{\pi}}\sqrt{\nu t} \approx 1.128\sqrt{\nu t} \tag{66}$$

Equation (66) accounts for the mean depth of penetration of the field to the potential region. Although the potential core is in a state of change, the process is still applicable, since we are interested in the characteristics of the boundary layer which is bounded by the surface and the potential core. In the case of momentum transport, this boundary layer defines the total mass flow, $U\delta_m$, at any time which results from the impulsive motion of an infinite flat plate.

Using the above result in Eq. (53) gives:

$$\tau^* = \frac{2}{\sqrt{\pi}}\frac{P\mathcal{L}}{A}\sqrt{t^*} \tag{67}$$

In summary, the asymptotic analysis yields:

$$\left.\begin{aligned} u^* &= t^* \quad t^* \to 0 \\ u^* &= \frac{A/P}{\mathcal{L}Po_{\mathcal{L}}} \quad t^* \to \infty \end{aligned}\right\} \tag{68}$$

and

$$\left.\begin{aligned} \tau^* &= \frac{2PL}{\sqrt{\pi}A}\sqrt{t^*} \quad t^* \to 0 \\ \tau^* &= 1 \quad t^* \to \infty \end{aligned}\right\} \tag{69}$$

2.3.3. Compact models

These exact limits may now be combined using the asymptotic correlation method [12]. The models of interest may now be written in the following forms:

$$u^* = \left[(t^*)^n + \left(\frac{A/P}{\mathcal{L}Po_{\mathcal{L}}}\right)^n\right]^{1/n} \tag{70}$$

and

$$\tau^* = \left[\left(\frac{2PL}{\sqrt{\pi}A}\sqrt{t^*}\right)^p + 1\right]^{1/p} \tag{71}$$

The values of n and p may now be determined from comparisons with data obtained from the exact solutions for a number of geometries. The fitting parameters may be obtained by either applying Eqs. (70) and (71) at a single known point in the transition region or by using multiple points and minimizing the root mean square error. In the present work, the latter method is used to determine the fitting parameters.

When the hydraulic diameter is used as a characteristic length scale Eqs. (70) and (71) become:

$$u^* = \left[(t^*)^n + \left(\frac{1}{4Po_{D_h}}\right)^n\right]^{1/n} \tag{72}$$

and

$$\tau^* = \left[\left(\frac{8}{\sqrt{\pi}}\sqrt{t^*}\right)^p + 1\right]^{1/p} \tag{73}$$

Comparisons were made in [9] with four known analytical solutions: the plane channel, the circular tube, the rectangle, and the circular annulus. Each of these four geometries are closely related. The annulus contains as special limits the tube and the channel results, and the rectangle also contains the channel limit. We only consider the tube and channel results in this paper.

The solution for the plane channel [15] of width $2h$ is:

$$u(y,t) = \frac{\mathcal{G}h^2}{2}\left[\left(1 - \frac{y^2}{h^2}\right) - 4\sum_{n=1}^{\infty}\frac{\sin(\delta_n)}{\delta_n^3}\cos(\delta_n y/h) \times \exp\left(-\delta_n^2 \nu t/h^2\right)\right] \tag{74}$$

where

$$\delta_n = \frac{(2n-1)\pi}{2} \tag{75}$$

The exact solutions for mean wall shear and mean velocity are:

$$\overline{u} = \mathcal{G}h^2\left(\frac{1}{3} - 2\sum_{n=1}^{\infty}\frac{\exp\left(-\delta_n^2\nu t/h^2\right)}{\delta_n^4}\right) \tag{76}$$

and the shear stress may be calculated from:

$$\tau_w = \mu\mathcal{G}h\left(1 - 2\sum_{n=1}^{\infty}\frac{\exp\left(-\delta_n^2\nu t/h^2\right)}{\delta_n^2}\right) \tag{77}$$

Equations (76) and (77) have been used to generate data for comparisons to the proposed models. Over the range of $0.0001 < t^* < 10$, 50–200 terms were used in the series as required to achieve convergence. The optimal fitting parameter for u^* was found to be $n = -1.3$ with a root mean square error (RMS) of 6.03 percent. While for τ^* the value was found to be $p = -6$ with a 0.262 percent RMS. Graphical results are shown in Figs. 5 and 6.

The solution for the circular tube of diameter $2a$ was obtained by Szymanski [16] using the separation of variables method. The solution is widely discussed in many advanced level fluid texts [1,2,4,7]. The solution is:

$$u(r,t) = \frac{\mathcal{G}a^2}{4}\left[\left(1-\frac{r^2}{a^2}\right) - 8\sum_{n=1}^{\infty}\frac{J_o(\delta_n r/a)}{\delta_n^3 J_1(\delta_n)}\exp\left(-\delta_n^2\nu t/a^2\right)\right] \tag{78}$$

where δ_n are the positive roots of

$$J_0(\delta_n) = 0 \tag{79}$$

The mean velocity may be found by integrating over the cross-sectional area

$$\overline{u} = \mathcal{G}a^2\left(\frac{1}{8} - 4\sum_{n=1}^{\infty}\frac{\exp\left(-\delta_n^2\nu t/a^2\right)}{\delta_n^3}\right) \tag{80}$$

and the shear stress is found to be:

$$\tau_w = \mu\mathcal{G}a\left(\frac{1}{2} - 2\sum_{n=1}^{\infty}\frac{\exp\left(-\delta_n^2\nu t/a^2\right)}{\delta_n^2}\right) \tag{81}$$

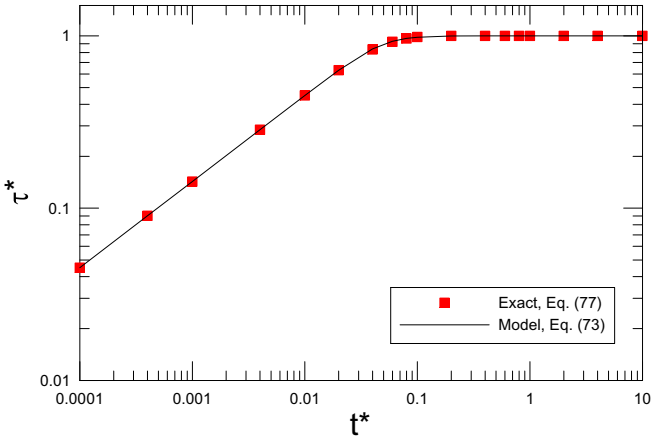

Fig. 6. τ^* for the Plane Channel.

Equations (80) and (81) have been used to generate data for comparisons to the proposed models. Over the range of $0.0001 < t^* < 10$, 50–200 terms were used in the series as required to achieve convergence. The optimal fitting parameter for u^* was found to be $n = -1.2$ with an RMS error of 6.94 percent. While for τ^* the value was found to be $p = -2.8$ with an RMS error of 2.72 percent. Graphical results are shown in Figs. 7 and 8.

The transition point for the dimensionless shear stress may be found from the intersection of the asymptotes in Eq. (73). This leads to $t^* \sim (\sqrt{\pi}/8)^2 \sim 0.0491$. Other solutions for the rectangular duct [9] and the annulus [17] are examined in [9].

2.4. Unsteady boundary layer flow

The unsteady development of laminar boundary layers has been considered by several researchers, see Rosenhead [1], Telionis [4] or Sherman [6]. This particular problem has been tackled using both approximate analytical and numerical methods. The problem under consideration is that of impulsively started stream over a semi-infinite flat plate. In time and space the flow progresses from a Stokes flow field to a Blasius flow field, as shown in Fig. 2.

The governing equations are continuity and the unsteady x-momentum equation:

$$\frac{\partial u}{\partial x} + \frac{\partial v}{\partial y} = 0 \tag{82}$$

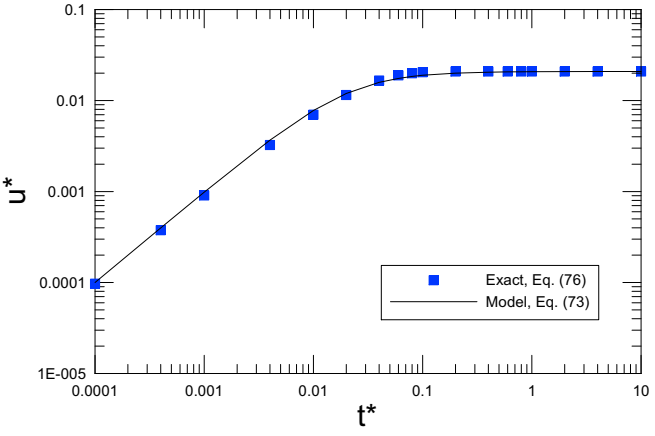

Fig. 5. u^* for the Plane Channel.

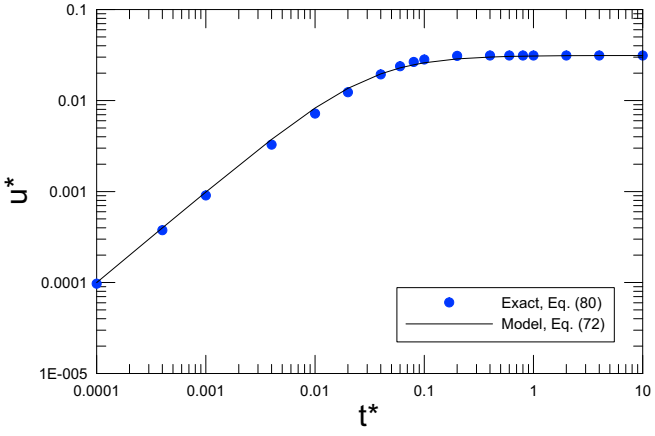

Fig. 7. u^* for the Circular Tube.

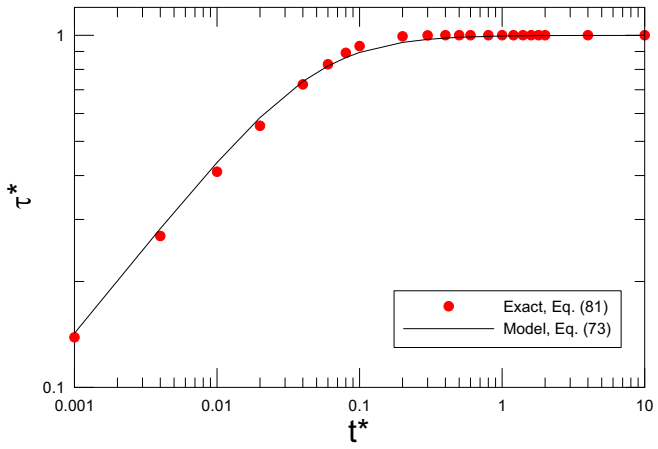

Fig. 8. τ^* for the Circular Tube.

and

$$\frac{\partial u}{\partial t}+u\frac{\partial u}{\partial x}+v\frac{\partial u}{\partial y}=\nu\frac{\partial^2 u}{\partial y^2} \tag{83}$$

which are subject to the following boundary and initial conditions:

$$\left.\begin{array}{ll} y=0 & u,v=0\\ y\to\infty & u=U\\ x=0 & u=U\\ t=0 & u=0 \end{array}\right\} \tag{84}$$

As we shall see, an important parameter in the solution of this problem is the grouping:

$$\frac{Ut}{x}=\frac{1}{St} \tag{85}$$

where St is one form of the Strouhal number [4]. The characteristics of this problem are such that at long times, $Ut/x >> 1$, the flow is steady and the wall shear is governed by Blasius flow. For short times, $Ut/x << 1$, the flow is unsteady and wall shear is obtained from Stokes flow. Conversely, similar characteristics are obtained when x is small, i.e. near the leading edge, $Ut/x >> 1$, and when x is large, i.e. downstream from the leading edge, $Ut/x << 1$.

A connection between Stokes flow and Blasius flow was first illustrated by Rayleigh [1]. Rayleigh [1] suggested that the Blasius problem could be modelled using an Oseen approximation whereby for steady flows, Eq. (83) could be replaced by

$$U\frac{\partial u}{\partial x}=\nu\frac{\partial^2 u}{\partial y^2} \tag{86}$$

which may be written as Eq. (3) if $t = x/U$. This leads to the solution for linearized Blasius problem of the form

$$\frac{u(\eta)}{U}=\operatorname{erf}\left(\frac{y}{2\sqrt{\nu x/U}}\right) \tag{87}$$

If we consider the effective residence time defined by $t = x/U$, the drag co-efficient becomes:

$$C_{f,x}=\frac{2}{\sqrt{\pi}}\sqrt{\frac{\mu}{\rho Ux}}=\frac{1.128}{\sqrt{Re_x}} \tag{88}$$

which over predicts laminar boundary layer theory, which yields a constant 0.664. Rayleigh suggested that $t = x/0.346U$ with no proof. This value of the effective time gives a constant 0.6638. A more general approach can be taken by linearizing the laminar boundary layer equations by formally defining an effective velocity [18]. This approach gives a similar value for the effective residence time as obtained by Rayleigh, but with a more formal approach.

Using the equations for unsteady boundary layer flow, the correct asymptotic characteristics will be obtained, and a simple model developed for the shear stress.

2.4.1. Scale analysis

Application of scaling analysis to Eqs. (82) and (83) yields several important characteristics. First, the continuity equation gives the transverse velocity scale:

$$v\sim\frac{U\delta}{x} \tag{89}$$

For short times, we may neglect the inertia terms in Eq. (83) and we obtain:

$$\delta_0\sim\sqrt{\nu t} \tag{90}$$

and

$$\tau_0\sim\frac{\mu U}{\delta_0} \tag{91}$$

while for long times, we neglect the transient term, and obtain:

$$\delta_\infty\sim\sqrt{\frac{\nu x}{U}} \tag{92}$$

and

$$\tau_0\sim\frac{\mu U}{\delta_\infty} \tag{93}$$

Finally, we see that the ratio of the short time and long time boundary layer thicknesses yields:

$$\frac{\delta_0}{\delta_\infty}\sim\sqrt{\frac{Ut}{x}} \tag{94}$$

If we define a dimensionless shear stress according to τ/τ_0 we then obtain the following dimensionless scales:

$$\left.\begin{array}{ll} \tau_0^*\sim 1 & \dfrac{Ut}{x}\to 0\\ \tau_0^*\sim\sqrt{\dfrac{Ut}{x}} & \dfrac{Ut}{x}\to\infty \end{array}\right\} \tag{95}$$

2.4.2. Asymptotic analysis

Stewartson [19] obtained an approximate solution to the unsteady boundary layer flow by linearizing the momentum equation using an Oseen approximation. The results were given as piecewise solution:

$$\left.\begin{array}{ll} u=U\operatorname{erf}\left(\dfrac{y}{2\sqrt{\nu t}}\right) & \dfrac{Ut}{x}<1\\ u=U\operatorname{erf}\left(\dfrac{1}{2}y\sqrt{\dfrac{U}{\nu x}}\right) & \dfrac{Ut}{x}>1 \end{array}\right\} \tag{96}$$

These approximate results illustrate how the flow transitions from a Stokes flow to a Blasius flow. However, this approximation is only valid near the leading edge of the plate. Stewartson [19] also obtained solutions using the momentum integral equation. Stewartson's [19] results for the wall shear were found to be in good agreement with the limits of Stokes flow and Blasius flow:

$$\left.\begin{array}{ll} \tau_w=0.534\rho U\sqrt{\nu/t} & \dfrac{Ut}{x}\le 2.65\\ \tau_w=0.328\rho U\sqrt{U\nu/x} & \dfrac{Ut}{x}\ge 2.65 \end{array}\right\} \tag{97}$$

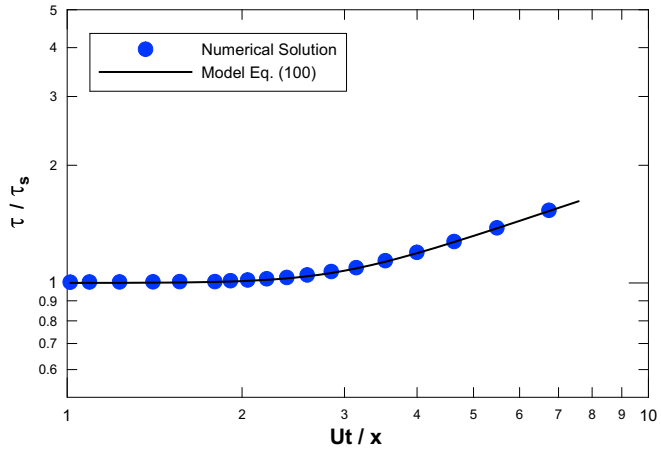

Fig. 9. τ^* for Unsteady Boundary Layer Flow.

These results show abrupt transition from one type of flow to the other. In fact this transition is not as abrupt and generally occurs in the range of $2 < \sqrt{Ut/x} < 4$. We may now examine the exact asymptotes for the wall shear using:

$$\left.\begin{aligned} \tau_0 &= 0.565\rho U\sqrt{\nu/t} \quad \frac{Ut}{x} \le 2.65 \\ \tau_\infty &= 0.332\rho U\sqrt{U\nu/x} \quad \frac{Ut}{x} \ge 2.65 \end{aligned}\right\} \tag{98}$$

The approximate transition point may be obtained by equating the two asymptotes, $\tau_0 \sim \tau_\infty$, to obtain $Ut/x \sim 2.90 \sim 3$. We may also define a dimensionless wall shear $\tau^* = \tau/\tau_0$. This leads to the following dimensionless asymptotes:

$$\left.\begin{aligned} \tau_0^* &= 1 \quad \frac{Ut}{x} \le 3 \\ \tau_\infty^* &= 0.587\sqrt{\frac{Ut}{x}} \quad \frac{Ut}{x} \ge 3 \end{aligned}\right\} \tag{99}$$

2.4.3. Compact models

These asymptotes may be combined using Eq. (1) with $n \approx 11$, in the form

$$\tau^* = \left[1 + \left(0.587\sqrt{\frac{Ut}{x}}\right)^{11}\right]^{1/11} \tag{100}$$

The accompanying plot in Fig. 9, shows the nature of the transition from Stokes flow to Blasius flow. The data points were obtained using the procedure outlined in Sherman [6] and Dwyer [20]. Comparison of the above model with the numerical data yields $n \approx 11$. This simple robust model provides a means to establish the transient response for a semi-infinite plate subjected to an impulsively started stream.

3. Summary and conclusions

The present work re-examined three fundamental unsteady viscous flow problems: unsteady Couette flow, unsteady Poiseuille flow, and unsteady boundary layer flow. Their link to Stokes's first problem was established by means of scaling and asymptotic analysis. Asymptotic results were combined using the Churchill–Usagi [12] method, to develop robust compact models for the dimensionless mean wall shear stress. These new models provide accurate results and an alternative to using more complex series solutions or graphical results.

Acknowledgments

The authors acknowledge the financial support of the Natural Sciences and Engineering Research Council of Canada (NSERC) under the Discovery grants program. The first author also acknowledges the assistance of Karl Lawrence, who re-solved the unsteady boundary layer flow problem numerically to provide the data in Fig. 9.

References

[1] L. Rosenhead, Laminar Boundary Layers. Dover, Publishing, New York, NY, 1959, pp. 349–408.
[2] H. Schlichting, Boundary Layer Theory. McGraw-Hill, New York, NY, 1979, pp. 90–93.
[3] I.G. Currie, Fundamental Mechanics of Fluids. McGraw-Hill, New York, NY, 1993, pp. 224–228.
[4] D.P. Telionis, Unsteady Viscous Flows. Springer-Verlag, 1981, pp. 79–102.
[5] R.L. Panton, Incompressible Flow. Wiley, 1995, pp. 166–172.
[6] F. Sherman, Viscous Flow. McGraw-Hill, New York, NY, 1991, pp. 335–336.
[7] F.M. White, Viscous Fluid Flow. McGraw-Hill, New York, NY, 1991, pp. 132–143.
[8] G.K. Batchelor, Introduction to Fluid Dynamics. Cambridge University Press, 1970, pp. 193–195.
[9] Y.S. Muzychka, M.M. Yovanovich, Compact models for transient conduction or viscous transport in non-circular geometries with a uniform source. International Journal of Thermal Sciences 45 (11) (2006) 1091–1102.
[10] A. Bejan, Convection Heat Transfer. Wiley, 1995.
[11] L.G. Leal, Laminar Flow and Convective Transport Processes. Butterworth-Heinemann, Boston, MA, 1992, pp. 91.
[12] S.W. Churchill, R. Usagi, A general expression for the correlation of rates of transfer and other phenomena. American Institute of Chemical Engineers 18 (1972) 1121–1128.
[13] M.M. Yovanovich, Asymptotes and Asymptotic Analysis for Development of Compact Models for Microelectronics Cooling. Keynote Address, Semitherm, San Jose, CA, March 2003.
[14] S.W. Yuan, Foundations of Fluid Mechanics. Prentice-Hall, 1967, pp. 291–293.
[15] H. Lamb, A Paradox in fluid motion. Journal of the London Mathematical Society 2 (1927) 109–112.
[16] P. Szymanski, Quelques Solutions Exactes des Equations de l'Hydrodynamique du Fluide Visqueux dans le Cas d'un Tube Cylindrique. Journal Mathematique Pure et Appliquee 11 (1932) 67–107.
[17] W. Müller, Zum Problem der Anlaufstromung einer Flussigkeit im geraden Rohr mit Kreisring und Kreisquerschnitt. ZAMM 16 (1936) 227–238.
[18] M.M. Yovanovich, S. Lee, T. Gayowsky, Approximate analytic solution of laminar forced convection from an isothermal plate, in: AIAA Paper 92-0248, 30th Aerospace Sciences Meeting and Exhibit, January 6–9, Reno, NV, 1992.
[19] K. Stewartson, On the impulsive motion of a Flate plate in a viscous fluid. Quarterly Journal of Mechanics 4 (1951) 182–198.
[20] H.A. Dwyer, Calculation of unsteady leading edge boundary layers. AIAA Journal 6 (1968) 2447–2448.